Available online at www.sciencedirect.com
ScienceDirect
Journal of Sound and Vibration 311 (2008) 408–420
JOURNAL OF SOUND AND VIBRATION
www.elsevier.com/locate/jsvi

In-plane and out-of-plane motions of an extensible semi-circular pipe conveying fluid

Duhan Jung[a], Jintai Chung[b,*]

[a]Department of Precision Mechanical Engineering, Graduate School, Hanyang University, 17 Haengdang-dong, Seongdong-gu, Seoul 133-791, Republic of Korea
[b]Department of Mechanical Engineering, Hanyang University, 1271 Sa-1-dong, Ansan, Kyunggi-do 425-791, Republic of Korea

Received 29 March 2007; received in revised form 13 September 2007; accepted 15 September 2007
Available online 22 October 2007

Abstract

In-plane and out-of-plane motions of a semi-circular pipe conveying fluid are analyzed in this paper. Assuming that the centerline of the semi-circular pipe is extensible, nonlinear equations of in-plane and out-of-plane motions are derived according to the extended Hamilton principle. The Lagrange nonlinear strain theory and the Euler–Bernoulli beam theory are used to derive the equations. The derived equations of motion are discretized by applying the Galerkin method. Linearized equations around the equilibrium position are obtained from the discretized equations, and then the dynamic characteristics of the pipe are investigated. In addition, some modelling issues, which are related to the nonlinearity of the circumferential strain and stress, are discussed. This study finds that a semi-circular pipe conveying fluid does not lose stability even at a high fluid velocity. Although a model using the Lagrange nonlinear strain and the corresponding nonlinear stress yields the most accurate computational results of the natural frequencies, a model using the Lagrange strain and a linearized stress is recommended to compute the natural frequencies efficiently while still maintaining accuracy.

1. Introduction

Vibration analyses of pipes conveying fluid have attracted the attention of many researchers, because the pipes are used in many industrial applications including heat-exchangers, refrigerators, air-conditioners, chemical plants and hydropower systems. Many studies have investigated nonlinear dynamics and stabilities of straight pipes conveying fluid [1–6]. In contrast, there are significantly fewer studies on curved pipes.

Chen [7,8] proposed an early dynamic model for the vibration analysis of a curved pipe conveying fluid. In his papers, the equations of in-plane and out-of-plane motions for a curved pipe were derived under the assumption that a pipe centerline is inextensible. Chen claimed that the dynamic characteristics of a curved pipe are similar to those of a straight pipe. Hill and Davis [9] derived the equations of motion to study the effects of initial forces on the stabilities of curved pipes. They found that the dynamical instabilities do not exist in a curved pipe when the pipe centerline is extensible. On the other hand, Misra et al. [10,11] studied the

*Corresponding author. Tel.: +82 31 400 5287; fax: +82 31 406 5550.
E-mail address: jchung@hanyang.ac.kr (J. Chung).

0022-460X/$ - see front matter © 2007 Elsevier Ltd. All rights reserved.
doi:10.1016/j.jsv.2007.09.011

differences of the dynamic characteristics between the curved pipes with *extensible* and *inextensible* centerlines. They concluded that a pipe model with an extensible centerline is more reasonable than a model with an inextensible centerline. Using a pipe model with an extensible centerline, Dupuis and Rousselet [12,13] derived nonlinear equations of motion for curved pipes conveying fluid with the consideration of the geometric nonlinearity and the infinitesimal strain simultaneously. However, the Lagrange nonlinear strain theory is more appropriate than the infinitesimal strain theory, because the infinitesimal strain is suitable for a linear system while the Lagrange strain is suitable for a nonlinear system. Adopting the Lagrange strain theory, Lee and Chung [14] presented a nonlinear model of a straight pipe conveying fluid. To the authors' knowledge, nonlinear equations of motion derived by considering nonlinearity with the Lagrange strain theory have not been reported for a curved pipe conveying fluid.

The in-plane and out-of-plane motions of a semi-circular pipe conveying fluid are analyzed in this paper. The semi-circular pipe is modelled as a curved Euler–Bernoulli beam with an extensible centerline. Since the pipe could undergo a large deformation at a high fluid velocity, the Lagrange strain theory is used to describe a nonlinear behavior due to the large deformation. After the nonlinear equations of motion are derived by applying the extended Hamilton principle [15], the equations of motion are discretized by the Galerkin method. Based on the linearized equations in the neighborhood of the equilibrium position, the natural frequencies of the semi-curved pipe are analyzed for the variation of fluid velocity. In addition, five models for the circumferential strain and stress are discussed, related to the nonlinearity of pipe.

2. Derivation of equations of motion

Consider a semi-circular pipe conveying fluid, as shown in Fig. 1, which is fixed at both ends. The semi-circular pipe has a centerline radius R, a cross-sectional outer diameter d_o and a wall thickness h. It is assumed that the pipe conveys an incompressible plug flow with a constant velocity U. To describe both the in-plane and out-of-plane motions of the pipe, two coordinate systems may be used: inertial and body-fixed. In Fig. 1, the XYZ coordinates are the inertial coordinates while the xyz coordinates are the body-fixed coordinates. The position of the body-fixed coordinate frame relative to the inertial coordinate frame is defined by the circumferential coordinate θ which is measured from the X-axis. The directions of the x and y axes coincide with the radial and tangential directions of the pipe centerline, respectively.

The displacements of a point in the pipe can be expressed by using the Euler–Bernoulli beam theory. The pipe can be modelled as an Euler–Bernoulli beam if it is sufficiently slender or the cross-sectional outer diameter d_o is much smaller compared to the centerline radius R. This means that the planar cross-section perpendicular to the y-axis remains a plane after deformation and the shear deformation in the yz plane is negligible. Denoting the x, y and z-directional displacements of an arbitrary point in the pipe by u_x, u_y and u_z, respectively, they may be represented in terms of the displacements of a point on the centerline and a twist angle about the y-axis:

$$u_x(z,\theta,t) = u(\theta,t) + z\phi(\theta,t), \quad u_y(x,z,\theta,t) = v(\theta,t) + x\phi_i(\theta,t) - z\phi_o(\theta,t)$$
$$u_z(x,\theta,t) = w(\theta,t) - x\phi(\theta,t), \tag{1}$$

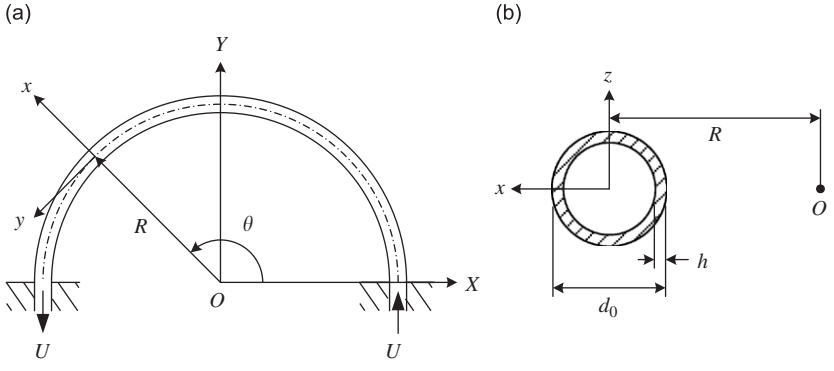

Fig. 1. Schematics of an extensible semi-circular pipe conveying fluid: (a) top view and (b) cross-section.

where t is time; u, v and w are displacements of a point on the centerline in the x, y and z directions; ϕ is a twist angle about the y-axis due to torsion; ϕ_i is a rotation angle about the z-axis due to in-plane bending deformation; and ϕ_o is a rotation angle about the x-axis due to out-of-plane bending. The rotation angles, ϕ_i and ϕ_o, due to in-plane and out-of-plane bending deformations are given by

$$\phi_i = (v - u')/R, \quad \phi_o = w'/R, \tag{2}$$

where the prime denotes the partial derivative with respect to θ [16].

To obtain the kinetic energy of the fluid-conveying pipe, velocities of both the pipe and the fluid need to be expressed in terms of the displacements u, v and w. The displacement vector of a point in the pipe after deformation can be written as

$$\mathbf{r} = (R + x + u_x)\mathbf{i} + u_y\mathbf{j} + (z + u_z)\mathbf{k}, \tag{3}$$

where $\mathbf{i}$, $\mathbf{j}$ and $\mathbf{k}$ are unit vectors along the x, y and z axes, respectively. Differentiation of Eq. (3) with respect to time leads to the pipe velocity

$$\mathbf{v}_p = \bar{\mathbf{v}}_p + x\boldsymbol{\omega}_i + z\boldsymbol{\omega}_o, \tag{4}$$

where

$$\bar{\mathbf{v}}_p = \dot{u}\mathbf{i} + \dot{v}\mathbf{j} + \dot{w}\mathbf{k}, \quad \boldsymbol{\omega}_i = (\dot{v} - \dot{u}')/R\mathbf{j} - \dot{\phi}\mathbf{k}, \quad \boldsymbol{\omega}_o = \dot{\phi}\mathbf{i} - \dot{w}'/R\mathbf{j}, \tag{5}$$

in which the superposed dot denotes differentiation with respect to time. Note that $\bar{\mathbf{v}}_p$ is the velocity of a point in the pipe centerline, $\boldsymbol{\omega}_i$ is the angular velocity about the z-axis, and $\boldsymbol{\omega}_o$ is the angular velocity about the x-axis. On the other hand, the material derivative of Eq. (3) results in the fluid velocity expressed by

$$\mathbf{v}_f = \bar{\mathbf{v}}_f + x\boldsymbol{\psi}_i + z\boldsymbol{\psi}_o, \tag{6}$$

where

$$\begin{aligned}
\bar{\mathbf{v}}_f &= [\dot{u} + U(u' - v)/R]\mathbf{i} + [\dot{v} + U(R + u + v')/R]\mathbf{j} + [\dot{w} + Uw'/R]\mathbf{k},\\
\boldsymbol{\psi}_i &= -(U/R)\dot{\phi}_i\mathbf{i} + [\dot{\phi}_i + (U/R)(1 + \phi_i')]\mathbf{j} - [\dot{\phi} + (U/R)\phi']\mathbf{k},\\
\boldsymbol{\psi}_o &= [\dot{\phi} + (U/R)(\phi' + \phi_o)]\mathbf{i} - [\dot{\phi}_o - (U/R)(\phi - \phi_o')]\mathbf{j}.
\end{aligned} \tag{7}$$

The detailed procedure to derive the above fluid velocity can be found in Ref. [17] which has been recently published. Since the circular pipe is assumed to be slender, the rotary inertia effects of the pipe about the x and z axes can be neglected. Therefore, the kinetic energy of the semi-circular pipe conveying fluid may be expressed as

$$T = \tfrac{1}{2}\int_0^{\pi} (m_p\bar{\mathbf{v}}_p \cdot \bar{\mathbf{v}}_p + I_p\dot{\phi}^2 + m_f\bar{\mathbf{v}}_f \cdot \bar{\mathbf{v}}_f)R\,\mathrm{d}\theta, \tag{8}$$

where m_p and m_f are pipe mass and fluid mass per unit length of pipe, respectively, and I_p is the polar mass moment of inertia about the y-axis per unit length of pipe:

$$I_p = \frac{m_p}{A}\int_A (x^2 + z^2)\,\mathrm{d}A, \tag{9}$$

where A is the cross-sectional area of the pipe.

The geometric nonlinearity due to large deformation of a beam can be generally described by the Lagrange strain theory [18], which describes nonlinear relations between the strains and the displacements. Based on the Lagrange strain theory, the circumferential normal strain at an arbitrary point in the pipe may be represented by

$$\varepsilon_y = \bar{\varepsilon}_y + x\phi_i'/R + z(\phi - \phi_o')/R + (\bar{\varepsilon}_y^2 + \phi_i^2 + \phi_o^2)/2, \tag{10}$$

where $\bar{\varepsilon}_y$ is the linear strain at a point on the pipe centerline given by

$$\bar{\varepsilon}_y = (u + v')/R. \tag{11}$$

Note that the first three terms in the right-hand side of Eq. (10) are linear while the last term is nonlinear.

Since the nonlinearity resulting from the shear deformation due to torsion is negligible, the shear strains can be expressed as linear combinations of displacements. Based on Ref. [19], the linear shear strains can be expressed as

$$\gamma_{xy} = z(\phi' + \phi_o)/R, \quad \gamma_{yz} = -x(\phi' + \phi_o)/R. \tag{12}$$

Next, consider the strain energy of the semi-circular pipe. It is assumed that the material of the pipe is homogeneous, isotropic, elastic and Hookean. Therefore, the stress–strain relations are given by

$$\sigma_x = E\varepsilon_x, \ \ \sigma_y = E\varepsilon_y, \ \ \sigma_z = E\varepsilon_z, \ \ \tau_{xy} = G\gamma_{xy}, \ \ \tau_{yz} = G\gamma_{yz}, \ \ \tau_{zx} = G\gamma_{zx}, \tag{13}$$

where E and G are Young's modulus and shear modulus, respectively. Since the outer radius d_o and the thickness h of the pipe are very small in comparison with the pipe radius R, stresses σ_x, σ_z and τ_{zx} can be neglected. In this case, the strain energy of the pipe may be expressed as

$$V = \frac{1}{2}\int_0^{\pi}\int_A (\sigma_y\varepsilon_y + \tau_{xy}\gamma_{xy} + \tau_{yz}\gamma_{yz})R\,\mathrm{d}A\,\mathrm{d}\theta, \tag{14}$$

where σ_y, τ_{xy} and τ_{yz} are the circumferential normal stress, radial shear stress and out-of-plane shear stress of the pipe, respectively.

The equations of motion and the associated boundary conditions for the semi-circular pipe conveying fluid are derived from the extended Hamilton principle [15]. For an open system with mass transport, the extended Hamilton principle is given by

$$\int_{t_1}^{t_2} (\delta T - \delta V + \delta W_{\mathrm{nc}} - \delta M)\,\mathrm{d}t = 0, \tag{15}$$

where δ is the variation operator, δW_{nc} is the virtual work done by non-conservative forces, and δM is the virtual momentum transport. The virtual work of this system is zero when non-conservative forces do not exist during free vibration of the pipe. On the other hand, since the pipe system has momentum transport of fluid at the boundaries, the virtual momentum transport should be considered. The virtual momentum may be expressed as

$$\delta M = m_f(\mathbf{v}_f \cdot \delta\mathbf{r})(U\mathbf{j}\cdot\mathbf{n})\big|_0^{\pi}, \tag{16}$$

where $\mathbf{n}$ is an outward normal unit vector at the boundaries. Introducing Eqs. (8), (14) and (16) into Eq. (15), the coupled nonlinear equations of motion are obtained as follows:

$$\begin{aligned}&(m_p + m_f)\ddot{u} + 2m_f U(\dot{u}' - \dot{v})/R + m_f U^2(u'' - u - 2v')/R^2 + EI(u^{iv} - v''')/R^4\\ &\quad + (EA/R)\{(1+\bar{\varepsilon}_y)(2\bar{\varepsilon}_y + \bar{\varepsilon}_y^2 + \phi_i^2 + \phi_o^2)/2 + [\phi_i(2\bar{\varepsilon}_y + \bar{\varepsilon}_y^2 + \phi_i^2 + \phi_o^2)/2]'\} = m_f U^2/R,\end{aligned} \tag{17}$$

$$\begin{aligned}&(m_p + m_f)\ddot{v} + 2m_f U(\dot{u} + \dot{v}')/R + m_f U^2(2u' + v'' - v)/R^2 + EI(u''' - v'')/R^4\\ &\quad - (EA/R)\{[(1+\bar{\varepsilon}_y)(2\bar{\varepsilon}_y + \bar{\varepsilon}_y^2 + \phi_i^2 + \phi_o^2)/2]' - \phi_i(2\bar{\varepsilon}_y + \bar{\varepsilon}_y^2 + \phi_i^2 + \phi_o^2)/2\} = 0,\end{aligned} \tag{18}$$

$$\begin{aligned}&(m_p + m_f)\ddot{w} + 2m_f U\dot{w}'/R + m_f U^2 w''/R^2 + EI(w^{iv} - R\phi'')/R^4\\ &\quad - (EA/R)[\phi_o(2\bar{\varepsilon}_y + \bar{\varepsilon}_y^2 + \phi_i^2 + \phi_o^2)/2]' - GJ(w'' + R\phi'')/R^3 = 0,\end{aligned} \tag{19}$$

$$I_p\ddot{\phi} - EI(w'' - R\phi)/R^3 - GJ(w'' + R\phi'')/R^2 = 0, \tag{20}$$

where I is the area moment of inertia about the x or z-axis and J is the polar area moment of inertia about the y-axis:

$$I = \int_A x^2\,\mathrm{d}A = \int_A z^2\,\mathrm{d}A, \quad J = \int_A (x^2 + z^2)\,\mathrm{d}A. \tag{21}$$

The associated boundary conditions are given by

$$u = u' = v = w = w' = \phi = 0 \ \text{ at } \ \theta = 0, \pi. \tag{22}$$

Eqs. (17)–(19) are for translation of the curved pipe conveying fluid while Eq. (20) is for torsional motion about the y-axis. Also noted that Eqs. (17)–(19) are nonlinear equations but Eq. (20) is a linear equation.

3. Discretization

Since exact solutions for Eqs. (17)–(20) cannot be found, the Galerkin method is used to obtain approximate solutions in a finite-dimensional function space. The displacements u, v and w as well as the twist angle ϕ may be represented by the trial functions that are expressed as a series of the basis functions. In this study, the basis functions are adopted as the comparison functions that satisfy both the essential and natural boundary conditions. The trial functions for u, v and w may be represented as

$$u(\theta,t)=\sum_{n=1}^{N}u_n(\theta)x_n^u(t),\quad v(\theta,t)=\sum_{n=1}^{N}v_n(\theta)x_n^v(t),\quad w(\theta,t)=\sum_{n=1}^{N}w_n(\theta)x_n^w(t) \tag{23}$$

and the trial function for ϕ can be written as

$$\phi(\theta,t)=\sum_{n=1}^{N}\phi_n(\theta)x_n^\phi(t), \tag{24}$$

where N is the total number of the basis functions; $u_n(\theta)$, $v_n(\theta)$, $w_n(\theta)$ and $\phi_n(\theta)$ are the basis function or the comparison functions; and $x_n^u(t)$, $x_n^v(t)$, $x_n^w(t)$ and $x_n^\phi(t)$ are unknown functions of time to be determined. The comparison functions are selected as the eigenfunctions of bending and axial vibrations for a straight beam:

$$\begin{aligned}u_n(\theta)&=w_n(\theta)=\cosh\,\lambda_n\theta-\cos\,\lambda_n\theta-\frac{\cosh\,\pi\lambda_n-\cos\,\pi\lambda_n}{\sinh\,\pi\lambda_n-\sin\,\pi\lambda_n}(\sinh\,\lambda_n\theta-\sin\,\lambda_n\theta)\\ v_n(\theta)&=\phi_n(\theta)=\sqrt{2}\,\sin\,n\theta,\end{aligned} \tag{25}$$

where λ_n are the roots of

$$\cosh\,\pi\lambda_n\cos\,\pi\lambda_n-1=0. \tag{26}$$

Note that the comparison functions satisfy the boundary conditions of Eq. (22). The weighting functions corresponding to the trial functions can be represented by

$$\begin{aligned}\bar{u}(\theta,t)&=\sum_{n=1}^{N}u_n(\theta)\bar{x}_n^u(t),\quad \bar{v}(\theta,t)=\sum_{n=1}^{N}v_n(\theta)\bar{x}_n^v(t),\quad \bar{w}(\theta,t)=\sum_{n=1}^{N}w_n(\theta)\bar{x}_n^w(t)\\ \bar{\phi}(\theta,t)&=\sum_{n=1}^{N}\phi_n(\theta)\bar{x}_n^\phi(t),\end{aligned} \tag{27}$$

where $\bar{x}_n^u(t)$, $\bar{x}_n^v(t)$, $\bar{x}_n^w(t)$ and $\bar{x}_n^\phi(t)$ are arbitrary functions of time.

The discretized equations can be obtained by substituting u, v, w and ϕ of Eq. (25) into Eqs. (17)–(20), multiplying these equations by $\bar{u}$, $\bar{v}$, $\bar{w}$ and $\bar{\phi}$ of Eq. (27) respectively, summing all the equations, integrating them over the domain of $0\leqslant\theta\leqslant\pi$, and then collecting all the terms with respect to $\bar{x}_n^u$, $\bar{x}_n^v$, $\bar{x}_n^w$ and $\bar{x}_n^\phi$. The coefficients of $\bar{x}_n^u$, $\bar{x}_n^v$, $\bar{x}_n^w$ and $\bar{x}_n^\phi$ provide a series of discretized equations. These equations may be expressed as the following nonlinear matrix-vector equation:

$$\mathbf{M}\ddot{\mathbf{x}}+2U\mathbf{G}\dot{\mathbf{x}}+(\mathbf{K}+U^2\mathbf{B})\mathbf{x}+\mathbf{N}(\mathbf{x})=U^2\mathbf{F}, \tag{28}$$

where $\mathbf{M}$ is the mass matrix, $\mathbf{G}$ is the matrix related to the gyroscopic force, $\mathbf{K}$ is the structural stiffness matrix, $\mathbf{B}$ is the matrix related to the centrifugal force, $\mathbf{N}$ is the nonlinear vector, $\mathbf{F}$ is the load vector due to flow, and $\mathbf{x}$ is the displacement vector given by

$$\mathbf{x}=\{x_1^u,x_2^u,\ldots x_N^u,\ x_1^v,x_2^v,\ldots x_N^v,\ x_1^w,x_2^w,\ldots x_N^w,\ x_1^\phi,x_2^\phi,\ldots x_N^\phi\}^{\mathrm{T}}. \tag{29}$$

4. Natural frequencies

To compute the natural frequencies of the semi-circular pipe conveying fluid, linearized equations should be obtained when the pipe is in a steady state. Using the perturbation method, the displacement vector can be expressed by

$$\mathbf{x} = \mathbf{x}_0 + \Delta\mathbf{x}, \tag{30}$$

where $\mathbf{x}_0$ is the vector for the equilibrium position, and $\Delta\mathbf{x}$ stands for small perturbation from the equilibrium position. When the pipe is in a steady state, the equilibrium position $\mathbf{x}_0$ is independent of time. Introduction of Eq. (30) into Eq. (28) leads to an equilibrium equation

$$(\mathbf{K} + U^2\mathbf{B})\mathbf{x}_0 + \mathbf{N}(\mathbf{x}_0) = U^2\mathbf{F} \tag{31}$$

and a linearized equation

$$\mathbf{M}\Delta\ddot{\mathbf{x}} + 2U\mathbf{G}\Delta\dot{\mathbf{x}} + (\mathbf{K} + \mathbf{K}_T + U^2\mathbf{B})\Delta\mathbf{x} = 0, \tag{32}$$

where $\mathbf{K}_T$ represents the tangential stiffness matrix at the equilibrium position:

$$\mathbf{K}_T = \left.\frac{\partial\mathbf{N}(\mathbf{x})}{\partial\mathbf{x}}\right|_{\mathbf{x}=\mathbf{x}_0}. \tag{33}$$

Since Eq. (31) is a nonlinear equation for $\mathbf{x}_0$, it should be solved by a nonlinear solver such as the Newton–Raphson method. The tangential stiffness matrix, given by Eq. (33), is determined after solving Eq. (31) for $\mathbf{x}_0$. Therefore, Eq. (32) describes a perturbed small motion in the neighborhood of the equilibrium position.

To obtain the natural frequencies of the pipe conveying fluid, the eigenvalue problem is derived by assuming the solution of Eq. (32) as

$$\Delta\mathbf{x} = \mathbf{X}e^{i\omega_n t}, \tag{34}$$

where $i = \sqrt{-1}$; $\mathbf{X}$ is a vibration amplitude vector, and ω_n is the natural frequency. Substituting Eq. (34) into Eq. (32), the following eigenvalue problem can be obtained:

$$(\mathbf{K} + \mathbf{K}_T + U^2\mathbf{B} - \omega_n^2\mathbf{M} + 2i\omega_n U\mathbf{G})\mathbf{X} = 0. \tag{35}$$

The natural frequencies are obtained from the condition that Eq. (35) has nontrivial solutions. This condition is given by

$$\det(\mathbf{K} + \mathbf{K}_T + U^2\mathbf{B} - \omega_n^2\mathbf{M} + 2i\omega_n U\mathbf{G}) = 0. \tag{36}$$

The natural frequencies can be computed numerically from Eq. (36), if all the parameters are specified. In the computations of this study, the following material properties and dimensions are used: $\rho_p = 7800\,\mathrm{kg/m^3}$, $\rho_f = 1000\,\mathrm{kg/m^3}$, $E = 72\,\mathrm{GPa}$, $G = 27\,\mathrm{GPa}$, $R = 200\,\mathrm{mm}$, $d_o = 22.25\,\mathrm{mm}$ and $h = 1.6\,\mathrm{mm}$. For convenience of comparison, a dimensionless natural frequency $\bar{\omega}$ and a dimensionless fluid velocity $\bar{U}$ are introduced as follows:

$$\bar{\omega}_n = \omega_n R^2\sqrt{\frac{m_p + m_f}{EI}}, \quad \bar{U} = UR\sqrt{\frac{m_f}{EI}}. \tag{37}$$

The convergence characteristics are investigated for the natural frequencies of the semi-circular pipe conveying fluid. The convergence results for $\bar{U} = 0$ are presented in Table 1, where the two lowest natural frequencies for the in-plane and out-of-plane motions converge with the total number of basis functions. Moreover, the converged values agree well with the analytical values reported by Blevins [20]. The convergence of the natural frequencies is also examined when the fluid velocity is not zero. Analytical values of the natural frequencies are not available when the semi-circular pipe has non-zero fluid velocity. Therefore, only convergence characteristics when $\bar{U} = 2$ are demonstrated in Table 2. Similarly to Table 1, Table 2 shows that the natural frequencies converge fast with the number of basis functions. Tables 1 and 2 show that

Table 1
Convergence characteristics of the two lowest dimensionless natural frequencies for the in-plane and out-of-plane motions when $\bar{U} = 0$

N	In-plane natural frequencies		Out-of-plane natural frequencies	
	$\bar{\omega}_1$	$\bar{\omega}_2$	$\bar{\omega}_1$	$\bar{\omega}_2$
1	54.6334	54.6712	2.0903	59.4277
2	28.2045	43.4818	2.0903	5.5518
3	4.8841	31.2243	1.8467	5.5518
4	4.4889	10.1156	1.8467	5.2938
5	4.4147	9.8325	1.8258	5.2938
6	4.3973	9.6512	1.8258	5.2597
7	4.3840	9.6374	1.8207	5.2597
8	4.3825	9.6041	1.8207	5.2496
9	4.3797	9.6030	1.8189	5.2496
10	4.3795	9.5955	1.8189	5.2455
Ref. [15]	4.3849	9.6329	1.8211	–

Table 2
Convergence characteristics of the two lowest dimensionless natural frequencies for the in-plane and out-of-plane motions when $\bar{U} = 2$

N	In-plane natural frequencies		Out-of-plane natural frequencies	
	$\bar{\omega}_1$	$\bar{\omega}_2$	$\bar{\omega}_1$	$\bar{\omega}_2$
1	53.6913	55.7151	2.0138	59.4277
2	28.2088	43.5716	1.9475	5.9968
3	4.9020	31.2951	1.6937	5.6968
4	4.3228	10.5006	1.6785	5.4553
5	4.2563	9.8438	1.6616	5.4241
6	4.2273	9.7227	1.6593	5.3991
7	4.2161	9.6753	1.6552	5.3931
8	4.2126	9.6517	1.6545	5.3861
9	4.2102	9.6446	1.6531	5.3841
10	4.2096	9.6392	1.6528	5.3813

reasonably converged natural frequencies are obtained when $N = 10$. Therefore, ten basis functions are used for further computations of the natural frequencies.

The natural frequencies of the semi-curved pipe conveying fluid are investigated for the nonlinear model given by Eqs. (17)–(20). For this model, the dimensionless natural frequencies $\bar{\omega}_n$ versus the dimensionless fluid velocity $\bar{U}$ are shown in Fig. 2, where the solid lines represent the in-plane natural frequencies and the dotted lines represent the out-of-plane natural frequencies. As seen in Fig. 2, the in-plane natural frequencies when $\bar{U}$ is relatively large become smaller than the frequencies when $\bar{U} = 0$. However, the out-of-plane natural frequencies show a behavior different from those of in-plane natural frequencies. The out-of-plane natural frequencies have a tendency to increase with the fluid velocity. From this observation, it may be deduced that a relatively large value of the fluid flow in the semi-circular pipe decreases the in-plane natural frequencies and increases the out-of-plane natural frequencies. In other words, transportation of fast fluid flow imposes a softening effect to the in-plane motion of a circular pipe while it imposes a stiffening effect to the out-of-plane motion. To the authors' knowledge, research comparing the in-plane and out-of-plane natural frequencies for the nonlinear vibrations has not yet been published.

5. Nonlinear modelling

In this section, modelling issues are discussed related to the nonlinearity of the circumferential strain and stress. The main topic of this section is the effect of modelling on the in-plane and out-of-plane natural

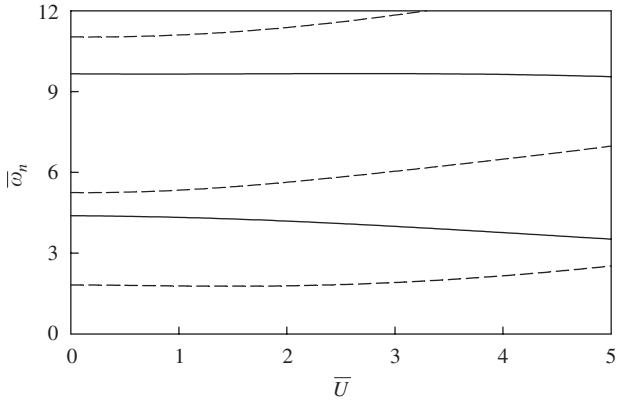

Fig. 2. Dimensionless natural frequencies $\bar{\omega}_n$ versus the dimensionless fluid velocity $\bar{U}$ for the nonlinear model of the semi-circular pipe conveying fluid. In-plane natural frequencies (solid line) and out-of-plane natural frequencies (dashed line).

frequencies. In this paper, the model of the circumferential strain and stress used to derive Eqs. (17)–(20) are called Model 1. In this model, the Lagrange nonlinear strain of Eq. (10) is adopted as the circumferential strain and the corresponding nonlinear stress is given by the second equation of Eq. (13). According to the von Karman strain theory, the quadratic term of the normal strain, $\bar{\varepsilon}_y^2$, is generally much smaller than the quadratic terms of the in-plane and out-of-plane rotations, ϕ_i^2 and ϕ_o^2. Neglecting the term $\bar{\varepsilon}_y^2$ in Eq. (10), the von Karman nonlinear strain is obtained as

$$\varepsilon_y = \bar{\varepsilon}_y + x\phi_i'/R + z(\phi - \phi_o')/R + (\phi_i^2 + \phi_o^2)/2. \tag{38}$$

Model 2 is defined by the nonlinear strain of Eq. (38) and the corresponding nonlinear stress. On the other hand, Model 3 uses the Lagrange nonlinear strain of Eq. (10) and a linearized stress

$$\sigma_y = E[\bar{\varepsilon}_y + x\phi_i'/R + z(\phi - \phi_o')/R] \tag{39}$$

and Model 4 uses the von Karman nonlinear strain of Eq. (38) and the linearized stress of Eq. (39). The model of strain and stress, which is similar to Model 4, can be found in Refs. [21,22], where the equations of motion for spinning disks are derived based on the von Karman strain and the linearized stress. Finally, Model 5 is defined by a linearized strain

$$\varepsilon_y = \bar{\varepsilon}_y + x\phi_i'/R + z(\phi - \phi_o')/R \tag{40}$$

and the linearized stress of Eq. (39). These five models are summarized in Table 3.

First, consider Model 5, because only this model yields linear equations of motion. Using this model, none of all the nonlinear terms appear in the equations of motion given by Eqs. (17)–(20). The dimensionless natural frequencies $\bar{\omega}_n$ of Model 5 are presented in Fig. 3 where the dimensionless fluid velocity $\bar{U}$ varies. Similarly to Fig. 2, the in-plane and out-of-plane natural frequencies are plotted as solid and dashed lines, respectively. The completely nonlinear case (Model 1) and the linear case (Model 5) show considerable differences in Figs. 2 and 3. As seen in Fig. 3, both the in-plane and out-of-plane natural frequencies decrease with the fluid velocity and they become zero at some specific values of fluid velocity. When the natural frequency has a zero value, the pipe system may begin to be unstable. The fluid velocity at which the natural frequency is zero is called the critical speed. If the fluid velocity is above the critical speed, the pipe system of Model 5 is subjected to instability such as divergence instability or flutter instability. In fact, the behaviors of the natural frequencies, as shown in Fig. 3, are quite similar to those of Chen [7,8]. However, Hill and Davis [9] claimed that a fluid-conveying circular pipe does not lose stability even in the case of a high fluid velocity if the centerline is extensible. For these reasons, it can be said that the linear model does not reflect real physical behavior and the nonlinearity should be taken into account in order to predict the behavior. Hence, there is no further discussion on Model 5 in this section.

Table 3
Five models for the circumferential strain and stress used to investigate the effects of the nonlinear terms on the natural frequencies

Model	Circumferential strain and stress	Remarks
Model 1	$\varepsilon_\theta = \bar{\varepsilon}_\theta + x\phi_i'/R + z(\phi - \phi_o')/R + (\bar{\varepsilon}_\theta^2 + \phi_i^2 + \phi_o^2)/2$	Lagrange nonlinear strain
	$\sigma_\theta = E[\bar{\varepsilon}_\theta + x\phi_i'/R + z(\phi - \phi_o')/R + (\bar{\varepsilon}_\theta^2 + \phi_i^2 + \phi_o^2)/2]$	Lagrange nonlinear stress
Model 2	$\varepsilon_\theta = \bar{\varepsilon}_\theta + x\phi_i'/R + z(\phi - \phi_o')/R + (\phi_i^2 + \phi_o^2)/2$	von Karman nonlinear strain
	$\sigma_\theta = E[\bar{\varepsilon}_\theta + x\phi_i'/R + z(\phi - \phi_o')/R + (\phi_i^2 + \phi_o^2)/2]$	von Karman nonlinear stress
Model 3	$\varepsilon_\theta = \bar{\varepsilon}_\theta + x\phi_i'/R + z(\phi - \phi_o')/R + (\bar{\varepsilon}_\theta^2 + \phi_i^2 + \phi_o^2)/2$	Lagrange nonlinear strain
	$\sigma_\theta = E[\bar{\varepsilon}_\theta + x\phi_i'/R + z(\phi - \phi_o')/R]$	Linearized stress
Model 4	$\varepsilon_\theta = \bar{\varepsilon}_\theta + x\phi_i'/R + z(\phi - \phi_o')/R + (\phi_i^2 + \phi_o^2)/2$	von Karman nonlinear strain
	$\sigma_\theta = E[\bar{\varepsilon}_\theta + x\phi_i'/R + z(\phi - \phi_o')/R]$	Linearized stress
Model 5	$\varepsilon_\theta = \bar{\varepsilon}_\theta + x\phi_i'/R + z(\phi - \phi_o')/R$	Linearized strain
	$\sigma_\theta = E[\bar{\varepsilon}_\theta + x\phi_i'/R + z(\phi - \phi_o')/R]$	Linearized stress

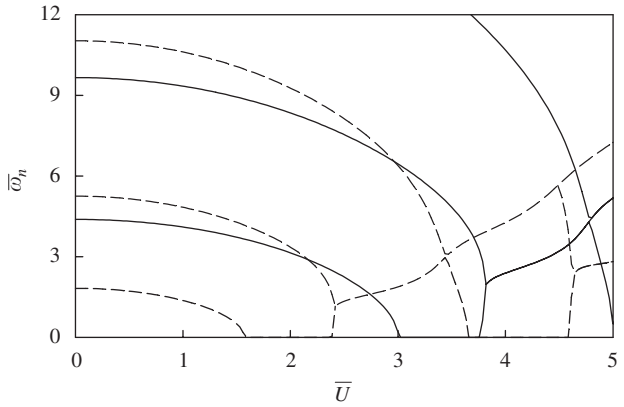

Fig. 3. Dimensionless natural frequencies $\bar{\omega}_n$ versus the dimensionless fluid velocity $\bar{U}$ for the linear model (Model 5) of the semi-circular pipe conveying fluid. In-plane natural frequencies (solid line) and out-of-plane natural frequencies (dashed line).

The in-plane and out-of-plane natural frequencies of the semi-circular pipe conveying fluid are investigated for Models 1–4, as shown in Table 3. For the variations of the dimensionless fluid velocity $\bar{U}$, the dimensionless natural frequencies $\bar{\omega}_n$ for the four models are presented in Figs. 4 and 5. Fig. 4 shows the in-plane natural frequencies while Fig. 5 shows the out-of-plane natural frequencies. In these figures, the solid, dashed, dotted and dash-dotted lines represent Models 1, 2, 3 and 4, respectively. From Figs. 4 and 5, it can be stated that, in general, all four models produce similar results at a very low fluid velocity. For example, when $\bar{U} = 0$, all the models have the same natural frequencies. However, the differences between some models become significant as $\bar{U}$ increases. These differences are due to the existence of geometric nonlinearities. Note that these effects in the semi-circular pipe could not be captured without considering the nonlinear terms of Eq. (10).

As shown in Figs. 4 and 5, there is no large difference between the natural frequencies obtained from Models 1 and 3. Table 4 compares the two lowest dimensionless natural frequencies when $\bar{U} = 5$ for Models 1–4. The numbers in parentheses of Table 4 are the differences of the natural frequencies between Model 1 and the other models. Table 4 and Figs. 4 and 5 demonstrate that the natural frequencies of Model 3 are the closest to those of Model 1, compared to Models 2 and 4. Therefore, Model 1 or 3 is suggested for predicting the natural frequencies at a high fluid velocity. Recall that Model 1 reflects full nonlinearities of the circumferential strain and stress while Model 3 reflects nonlinearity for the strain only. Since Model 3 requires less computational cost than Model 1, it is beneficial to use Model 3. In other words, in order to compute the

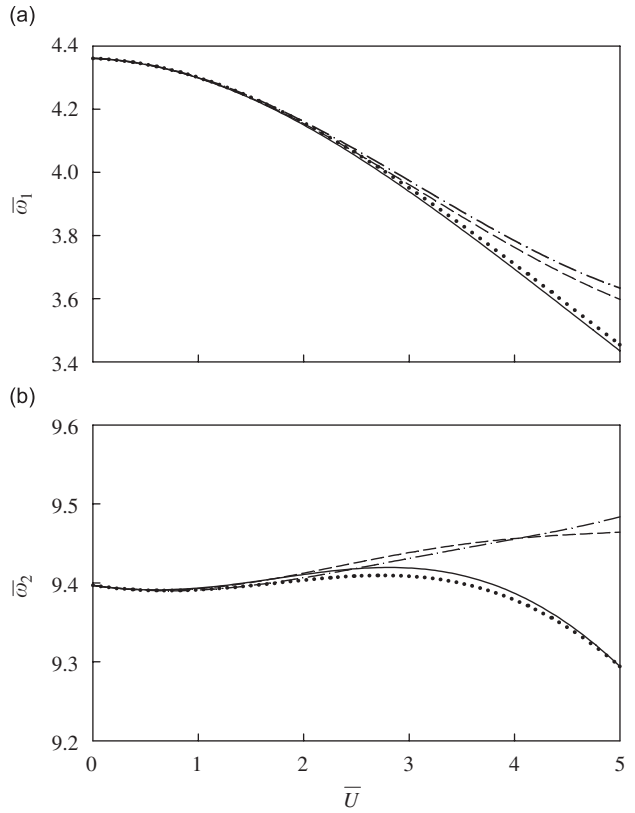

Fig. 4. Dimensionless in-plane natural frequencies $\bar{\omega}_n$ versus the dimensionless fluid velocity $\bar{U}$ for the four models of the semi-circular pipe conveying fluid: (a) first natural frequency and (b) second natural frequency. Model 1 (solid line), Model 2 (dashed line); Model 3 (dotted line) and Model 4 (dash-dot line).

natural frequencies of the semi-circular pipe accurately and efficiently, the Lagrange nonlinear strain and the linearized stress (Model 3) should be used to derive the equations of motion.

To show differences between the four models in a practical problem, the natural frequencies are considered for a circular pipe in a nuclear power plant. The material properties of the pipe are given by $E = 3.9786 \times 10^9\,\mathrm{N/m^2}$, $m_p = 0.1415\,\mathrm{kg/m}$ and $m_f = 0.3874\,\mathrm{kg/m}$ while the dimensions of the pipe are $R = 511\,\mathrm{mm}$, $d_0 = 25.375\,\mathrm{mm}$ and $h = 1.5875\,\mathrm{mm}$. Table 5 shows the fundamental natural frequencies for the circular pipe when $U = 20$ and $80\,\mathrm{m/s}$. In this table, $(f_n)_i$ and $(f_n)_o$ are the fundamental natural frequencies of the pipe for the in-plane and out-of-plane motions, respectively. The numbers in parentheses also mean the differences of the natural frequencies between Model 1 and the other models. As shown in Table 5, the natural frequencies do not have large differences between the four models when the fluid velocity is relatively low or when $U = 20\,\mathrm{m/s}$. However, if the velocity increases to $U = 80\,\mathrm{m/s}$, the natural frequency differences become large. As discussed before, it may be concluded that the computation results from Model 3 are not only accurate but they are also efficient.

6. Summary and conclusions

For a semi-circular pipe conveying fluid, the nonlinear equations of in-plane and out-of-plane motions are derived by using the extended Hamilton principle. During the derivation, the Lagrange strain theory is applied to consider the geometric nonlinearity of the semi-circular pipe. Furthermore, the extensibility of the pipe centerline is also considered. The derived equations consist of two nonlinear equations of in-plane motion, a nonlinear equation of out-of-plane motion and a linear equation of torsional motion. The equations of motion

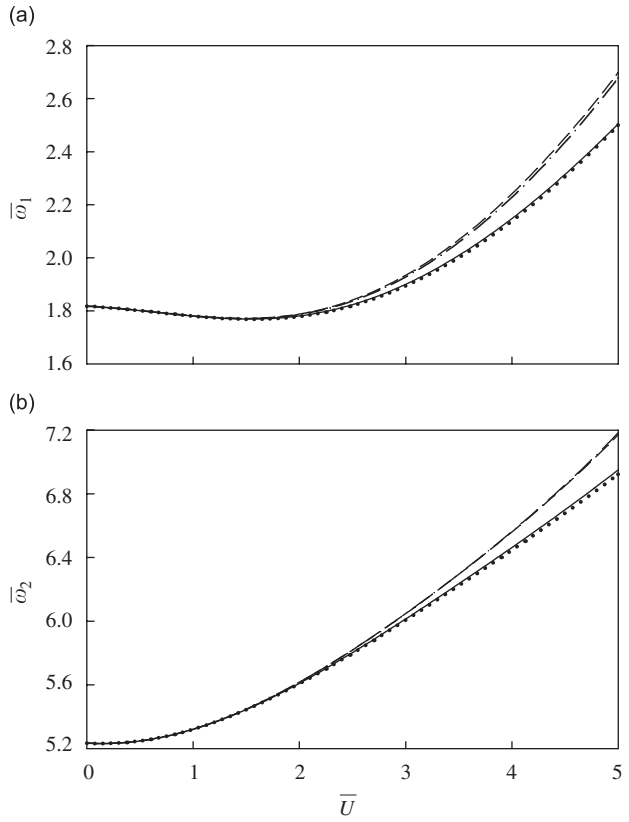

Fig. 5. Dimensionless out-of-plane natural frequencies $\bar{\omega}_n$ versus the dimensionless fluid velocity $\bar{U}$ for the four models of the semi-circular pipe conveying fluid: (a) first natural frequency and (b) second natural frequency. Model 1 (solid line); Model 2 (dashed line), Model 3 (dotted line) and Model 4 (dash-dot line).

Table 4
Comparison of the two lowest dimensionless natural frequencies for Models 1–4 when $\bar{U} = 5$

	In-plane natural frequencies		Out-of-plane natural frequencies	
	$\bar{\omega}_1$	$\bar{\omega}_2$	$\bar{\omega}_1$	$\bar{\omega}_2$
Model 1	3.4351	9.2944	2.5044	6.9497
Model 2	3.5976	9.4642	2.6971	7.1699
	(4.73%)	(1.83%)	(7.69%)	(3.17%)
Model 3	3.4545	9.2942	2.4995	6.9225
	(0.56%)	(−0.01%)	(−0.20%)	(−0.39%)
Model 4	3.6333	9.4836	2.6771	7.1815
	(5.77%)	(2.04%)	(6.90%)	(3.34%)

are discretized by applying the Galerkin method. The discretized equations are expressed as a nonlinear matrix–vector equation, from which the linearized equation around the equilibrium position is obtained to investigate the natural frequencies. In addition, some modelling issues, which are related to the nonlinearity of the circumferential strain and stress, are also discussed.

The results of this study can be summarized as follows:

(1) Fast fluid flow in a semi-circular pipe imposes a softening effect on the in-plane motion; however, it imposes a stiffening effect on the out-of-plane motion.

Table 5
Comparison of the fundamental natural frequencies for a semi-circular pipe in a nuclear plant

	$U = 20$ m/s		$U = 80$ m/s	
	$(f_n)_i$ (Hz)	$(f_n)_o$ (Hz)	$(f_n)_i$ (Hz)	$(f_n)_o$ (Hz)
Model 1	8.6375	20.8423	17.4802	11.0412
Model 2	8.6405	20.8436	17.9559	11.6535
	(0.04%)	(0.01%)	(2.72%)	(5.55%)
Model 3	8.6364	20.8523	17.5647	10.9979
	(−0.01%)	(0.05%)	(0.48%)	(−0.39%)
Model 4	8.6396	20.8538	18.0808	11.5762
	(0.03%)	(0.06%)	(3.44%)	(4.84%)

(2) A semi-circular pipe conveying fluid does not lose stability even for a high fluid velocity.
(3) At a low fluid velocity, none of the models (Models 1–5) produce large differences in the natural frequencies.
(4) At a high fluid velocity, the natural frequencies of the nonlinear models (Models 1–4) do not decrease to zero, but those of the linear model (Model 5) decrease to zero.
(5) Model 3 should be used to predict the natural frequencies accurately and effectively.

Acknowledgement

This study was supported by a grant (Grant no: R05-2003-000-10305) from the Korea Science and Engineering Foundation, Republic of Korea. This support is gratefully acknowledged.

References

[1] A.L. Thurman, C.D. Mote Jr., Non-linear oscillation of a cylinder containing flowing fluid, *Journal of Engineering for Industry* 91 (1969) 1147–1155.
[2] C. Semler, G.X. Li, M.P. Païdoussis, The non-linear equations of motion of pipes conveying fluid, *Journal of Sound and Vibration* 169 (1994) 577–599.
[3] U. Lee, C.H. Pak, S.C. Hong, The dynamics of a piping system with internal unsteady flow, *Journal of Sound and Vibration* 180 (1995) 297–311.
[4] C. Semler, M.P. Païdoussis, Non-linear analysis of the parametric resonances of a planar fluid-conveying cantilevered pipe, *Journal of Fluids and Structures* 10 (1996) 787–825.
[5] D.G. Gorman, J.M. Reese, Y.L. Zhang, Vibration of a flexible pipe conveying viscous pulsating fluid flow, *Journal of Sound and Vibration* 230 (2000) 379–392.
[6] M.P. Païdoussis, *Fluid–Structure Interactions: Slender Structures and Axial Flow*, Academic Press, New York, 1998.
[7] S.S. Chen, Vibration and stability of a uniformly curved tube conveying fluid, *Journal of Acoustical Society of America* 51 (1972) 223–232.
[8] S.S. Chen, Out-of-plane vibration and stability of curved tubes conveying fluid, *Journal of Applied Mechanics* 40 (1973) 362–368.
[9] J.L. Hill, C.G. Davis, The effect of initial forces on the hydrostatic vibration and stability of planar curved tubes, *Journal of Applied Mechanics* 41 (1974) 355–359.
[10] A.K. Misra, M.P. Païdoussis, K.S. Van, On the dynamics of curved pipes transporting fluid. Part I: inextensible theory, *Journal of Fluid and Structures* 2 (1988) 211–244.
[11] A.K. Misra, M.P. Païdoussis, K.S. Van, On the dynamics of curved pipes transporting fluid. Part II: extensible theory, *Journal of Fluid and Structures* 2 (1988) 245–261.
[12] C. Dupuis, J. Rousselet, The equations of motion of curved pipes conveying fluid, *Journal of Sound and Vibration* 153 (1992) 473–489.
[13] C. Dupuis, J. Rousselet, Hamilton's principle and the governing equations of fluid-conveying curved pipes, *Journal of Sound and Vibration* 160 (1993) 172–174.
[14] S.I. Lee, J. Chung, New non-linear modelling for vibration analysis of a straight pipe conveying fluid, *Journal of Sound and Vibration* 254 (2002) 313–325.
[15] D.B. McIver, Hamilton's principle for systems of changing mass, *Journal of Engineering Mathematics* 7 (1972) 249–261.
[16] S.S. Rao, V. Sundararajan, In-plane flexural vibrations of circular rings, *Journal of Applied Mechanics* 36 (1969) 620–625.
[17] D. Jung, J. Chung, H.H. Yoo, New fluid velocity expression in an extensible semi-circular pipe conveying fluid, *Journal of Sound and Vibration* 304 (2007) 382–390.

[18] J.J. Prescott, *Applied Elasticity*, Dover Publications, New York, 1967.
[19] S.Y. Lee, J.C. Chao, Out-of-plane vibrations of curved non-uniform beams of constant radius, *Journal of Sound and Vibration* 238 (2000) 443–458.
[20] R.D. Blevins, *Formulas for Natural Frequency and Mode Shape*, Van Nostrand Reinhold, New York, 1979.
[21] J. Chung, J.-E. Oh, H.H. Yoo, Non-linear vibration of a flexible spinning disc with angular acceleration, *Journal of Sound and Vibration* 231 (2000) 375–391.
[22] J.W. Heo, J. Chung, Vibration analysis of a flexible rotating disk with angular misalignment, *Journal of Sound and Vibration* 231 (2004) 821–841.